Sodium MRI using a density adapted 3D Radial Acquisition

A. M. Nagel[1], F. B. Laun[1], M-A. Weber[2], and L. R. Schad[3]

[1]Medical Physics in Radiology, German Cancer Research Center, Heidelberg, Germany, [2]Radiology, German Cancer Research Center, Heidelberg, Germany, [3]Computer Assisted Clinical Medicine, Faculty of Medicine Mannheim, University Heidelberg

Introduction

Sodium MRI has the potential to differentiate viable from non-viable tissue [1]. The *in vivo* ^{23}Na signal decays biexponentially, with a short component of T_{2s} = 0.5-8 ms and a long component of T_{2l} = 15-30 ms [2]. Therefore pulse sequences that enable short echo times like 3D Radial Projections Imaging (3D-RAD) [3], 3D-Cones acquisition (3D-Cones) [4] and Twisted Projection imaging (TPI) [5] have been used for sodium imaging. Furthermore sodium imaging requires SNR efficient acquisition techniques, due to low *in vivo* concentrations. TPI and 3D-Cones acquisition provide a sampling which is more efficient for the SNR compared to 3D-RAD at the cost of limitations in the sequence design parameters and a more complicated gradient switching. We implemented a density adapted 3D Radial sampling scheme (DA-3D-RAD) that combines the convenience of the radial trajectory with a more efficient k-space sampling. In this work sodium imaging with 3D-RAD acquisition was compared with the DA-3D-RAD acquisition.

Methods

A 3D-RAD imaging sequence was implemented as described in [3]. The gradients for the DA-3D-RAD acquisition have a trapezoidal form up to a time t_0. After this time the gradient amplitude decreases, such that the imaging time for each spherical shell (shells of the same thickness) of k-space is proportional to the shells surface. For a 3D radial acquisition the number of k-space samples in a shell with radius k is proportional to the inverse of the gradient strength G(k) and to the inverse of k^2 (1). The gradients for the DA-3D-RAD acquisition were designed in a way that for a k-space radius $k > k_0$ the number of k-space samples in all spherical shells is kept constant, which is equivalent to the constraint (2). Solving equation (2) leads to the form of the gradients (eq. 3; Fig. 1). The resulting radial k-space positions vs. time are shown in Fig. 2. Both sequences were implemented on a 3.0 T clinical MR system (Magnetom Tim Trio, Siemens Medical Solutions, Erlangen, Germany). Images were acquired using a double-resonant (32.59 MHz/ 123.2 MHz) birdcage coil (Rapid Biomed GmbH, Würzburg, Germany). Image reconstruction was performed offline with Matlab (Mathworks, Natick; MA, USA). A Kaiser-Bessel gridding kernel was used [6], followed by a conventional FFT without filtering. *In vivo* brain images, images of a resolution phantom, and images of a spherical phantom were acquired. The switching of the gradients is shown in Fig. 1 (DA-3D-RAD: t_0 = 0.5 ms; G_0 = 8.87 mT/m / 3D-RAD: G_0 = 1.11 mT/m). For both sequences the same parameters were used (TE = 0.2 ms; 10 ms readout window; resolution of 4x4x4 mm^3; 5000 projections). SNR measurements were performed *in vivo* and in phantom images, according to the NEMA definition [7]. The mean signal in selected ROI's was measured in each of the four images from every single repetition. The standard deviation in the ROI's was calculated from difference images.

$$(1)\quad D(k) \propto \frac{1}{4\pi k^2 G(k)}$$

$$(2)\quad \frac{1}{4\pi k^2 G(k)} = \frac{1}{4\pi k_0^2 G(k_0)}$$

$$(3)\quad G(t) = k_0^2 G_0 \left(\frac{3\gamma}{2\pi} k_0^2 G_0 (t - t_0) + k_0^3\right)^{-2/3} \quad for\ t \geq t_0$$

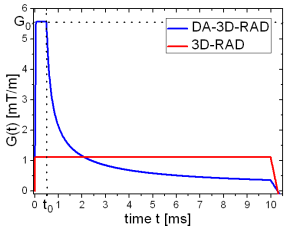

Fig. 1: Form of the gradients.

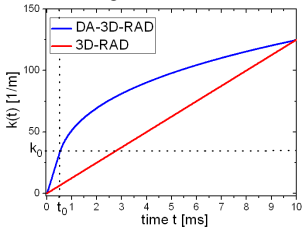

Fig. 2: Radial k-space position vs. time

Results

In vivo images show that the DA-3D-RAD sequence provides a better resolution of fine details (e.g. cerebrum, viscerocranium) and a better SNR (Fig. 3). The corresponding SNR/average values are listed in table 1. Fig. 4b (DA-3D-RAD) and Fig. 4c (3D-RAD) show images of a resolution phantom. In the spherical phantom SNR values of 9.5 (DA-3D-RAD) and 7.1 (3D-RAD) were measured. Both, phantom and *in vivo* measurements show a significantly higher SNR for the density adapted acquisition scheme (DA-3D-RAD) compared to the standard 3D-RAD sequence. Furthermore the DA-3D-RAD sampling scheme (Fig. 4b) gave a slightly better resolution compared to the 3D-RAD acquisition (Fig. 4c).

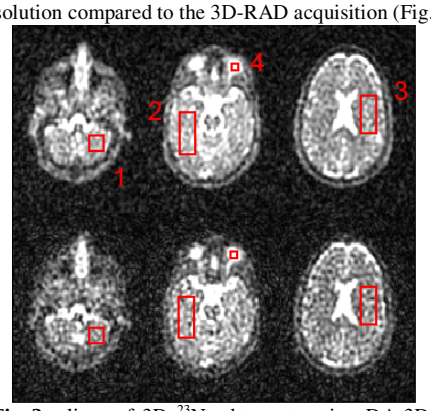

Fig. 3: slices of 3D ^{23}Na data sets using DA-3D-RAD (top) and 3D-RAD (bottom). (TE/TR = 0.2/60 ms; 4 averages)

	ROI 1	ROI 2	ROI 3	ROI 4
DA-3D-RAD	3.9 ± 0.3	4.2 ± 0.2	4.5 ± 0.2	9.60 ± 1.6
3D-RAD	2.5 ± 0.2	2.8 ± 0.1	3.0 ± 0.2	7.8 ± 2.3
Ratio	1.6	1.5	1.5	1.2

Table 1: Comparison of SNR/averaging values in ROI's shown in Fig. 3. SNR was measured according to the NEMA definition [7].

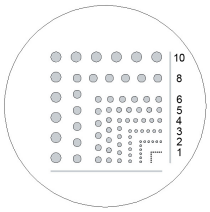

Fig. 4a: resolution phantom; sizes of the rods are given in mm

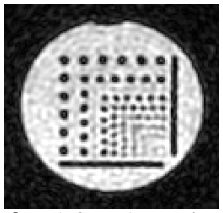

Fig. 4b: DA-3D-RAD Na-images of the resolution phantom (TE/TR = 0.2/100 ms; 2 averages)

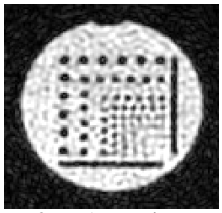

Fig. 4c: 3D-RAD Na-images of the resolution phantom (TE/TR = 0.2/100 ms; 2 averages)

Discussion

Improved resolution which is achieved with the density adapted sequence can be attributed to a more efficient sampling of the higher k-space frequencies and lower image noise. The density adapted gradients have a closed analytical form providing a more flexible sequence design in combination with SNR efficient k-space sampling. Therefore in SNR limited applications such as sodium imaging the DA-3D-RAD acquisition is an alternative to 3D-Cones or TPI sampling schemes and performs better than the 3D-RAD sequence.

References

[1] Kim R.J. et al. ; Circulation 95 (1997); 1877-79
[2] Constantinides et al.; Radiology (2000); 216: 559-568
[3] Nielles-Vallespin et al.; MRM (2007); 57: 74-81
[4] Gurney et al.; MRM (2006); 55: 575–582
[5] Boada et al.; MRM (1997); 37: 706-715
[6] Jackson et al. IEEE Transactions on Medical Imaging; (1991 10(3)); 473-478
[7] NEMA Standards publication MS 1-2001